White Matter Lesion Segmentation from Volumetric MR Images

Faguo Yang[1,2], Tianzi Jiang[2], Wanlin Zhu[2], and Frithjof Kruggel[1]

[1] Max-Planck Institute of Cognitive Neuroscience
Stephanstrasse 1A, 04103 Leipzig, Germany
[2] National Lab of Pattern Recognition, Institute of Automation
Chinese Academy of Sciences, Beijing 100080, China.
{fgyang, jiangtz, wlzhu}nlpr.ia.ac.cn

Abstract. White matter lesions are common pathological findings in MR tomograms of elderly subjects. These lesions are typically caused by small vessel diseases (e.g., due to hypertension, diabetes). In this paper, we introduce an automatic algorithm for segmentation of white matter lesions from volumetric MR images. In the literature, there are methods based on multi-channel MR images, which obtain good results. But they assume that the different channel images have same resolution, which is often not available. Although our method is also based on T1 and T2 weighted MR images, we do not assume that they have the same resolution (Generally, the T2 volume has much less slices than the T1 volume). Our method can be summarized as the following three steps: 1) Register the T1 image volume and the T2 image volume to find the T1 slices corresponding to those in the T2 volume; 2) Based on the T1 and T2 image slices, lesions in these slices are segmented; 3) Use deformable models to segment lesion boundaries in those T1 slices, which do not have corresponding T2 slices. Experimental results demonstrate that our algorithm performs well.

1 Introduction

White matter lesions are common pathological findings in MR tomograms of elderly subjects, which are typically caused by small vessel diseases (e.g., due to hypertension, diabetes). It is currently under debate how much the presence of these lesions is related to cognitive deficits in elderly subjects. So an automatic analysis is very useful. But building reliable tools to segment MR images with pathological findings is a nontrivial task. Manual segmentation is a fundamental way to segment MR images, but it takes a trained specialist a lot of time because of the large amount of image data. Moreover, different specialists may give different segmentation results. Compared with manual segmentation, the advantages of automatic segmentation include increased reliability, consistency, and reproducibility.

In the literature, several brain lesion segmentation methods have been introduced [1,2,3,4,5,6,7], and many of them concentrate on multiple sclerosis

G.-Z. Yang and T. Jiang (Eds.): MIAR 2004, LNCS 3150, pp. 113–120, 2004.

(MS)[3,4,7]. Some of these algorithms use only T1-weighted images [5,6], others are based on multi-channel volumes [1,3,4]. In [1], a semi-automatic method is introduced, in which typical tissue voxels (white matter, cerebral spinal fluid, and gray matter, lesions) are selected by the user to train an artificial network, then it is used to analyze the MR images; Leemput, et al. [3] view lesions as outliers and use a robust parameter estimation method to detect them. A multi-resolution algorithm is used to detect Multiple Sclerosis lesions in [4]. Kovalev, et al. [5] take advantage of texture analysis to extract features for description of white matter lesions. In [7], models of normal tissue distribution are used for brain lesion segmentation, but they label lesions in the transformed data space, instead of the original image volume.

The main obstacle to white matter lesion segmentation is that the intensities of white matter lesions and gray matter are very similar in T1-weighted images , therefore they can not be distinguished only by intensities of the T1 images (see Fig. 1). It is expected that multi-channel based methods will obtain better results. On most current scanners, it takes an inacceptable long time to acquire a T2-weighted image volume at the same resolution as a T1-weighted volume, that is approximately 1 mm in all spatial directions. Thus, most imaging protocols only allow for the acquisition of a sparse set (20-30) of T2-weighted slices at a typical slice thickness of 5-7 mm. The aim of this paper is to develop a white matter lesion segmentation algorithm based on multi-channel MR volumes, but we do not assume that T1 volumes and T2 volumes have the same resolution. Our algorithm can be summarized as follows: 1) Register the T1 image volume and the T2 image volume to find the T1 slices corresponding to those in the T2 volume; 2) Based on the T1 and T2 image slices, lesions in these slices are segmented; 3) Use deformable models to segment lesion borders in those T1 slices, which do not have corresponding T2 slices. The deformable model is initialized according to the neighboring segmented lesions based on both T1 and T2 slices.

The rest of the paper is organized as follows: Section 2 is devoted to the segmentation of lesions based on both T1 image and T2 image slices. We describe how to apply deformable models for lesion segmentation in Section 3; Experimental results are given in Section 4; A summary is made in Section 5.

2 Lesion Segmentation Based on T1 and T2 Slices

As for the T1 image volume and the T2 image volume are of the same person and are scanned almost in the same time, registration methods based on rigid transformation are enough for our requirements. We use the registration method [8] to find which T1 slices correspond to those T2 slices. And these T1 slices form a T1 volume denoted by S with the same resolution as the T2 volume. At the same time, the T1 volume is transformed using the same transformation parameters.

We firstly segment lesions in those T1 weighted slices that have corresponding T2 slices. These segmented lesions provide some location and shape information

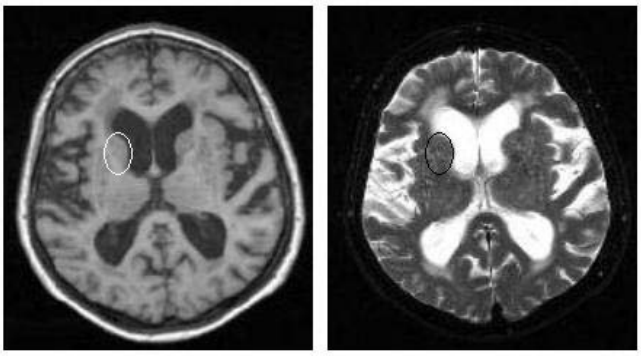

Fig. 1. Illustration of image parts, which can not be distinguished only by T1 image.

of the lesions in other slices. The steps to segment lesions based on T1 and T2 slices are as follows:

- Both the selected T1 image volume S and the T2 volume are segmented using a C-fuzzy mean algorithm [9]. Only those voxels, which are similar with gray matter in T1 channel and similar with CSF in T2 channel are classified as lesions. This can be expressed as follows:

$$\Gamma_{les} = \{v | p_{v,gm}(T1) p_{v,csf}(T2) > \beta\} \tag{1}$$

  where $p_{v,gm}(T1)$ and $p_{v,csf}(T2)$ are the memberships indicating in how much context voxel v belongs to gray matter in T1 volume and belongs to CSF in T2 volume, respectively.
- From the segmented lesions, we can obtain some statistical lesion information (mean value μ_{les} and standard deviation σ_{les}).

Some slices of the T2 image volume, its corresponding T1 slices and the segmented lesions are shown in Fig. 2.

3 Lesion Segmentation by Applying Deformable Models

Following the lesion segmentation in the corresponding slices, it is necessary to process those slices without corresponding T2 slices. We assume that the lesions in neighboring T1 slices are similar, that is, the location and shape of the lesions does not greatly vary. This is likely, when the T1 volume resolution in the slice direction is high (our image data is 1mm) and the lesions are not very small. We can make use of the the location and shape information obtained from the segmented lesions based on both weightings. We use deformable models to accomplish this task. The deformable model is firstly initialized by the neighboring segmented lesions, then adapts itself according to the current image slice.

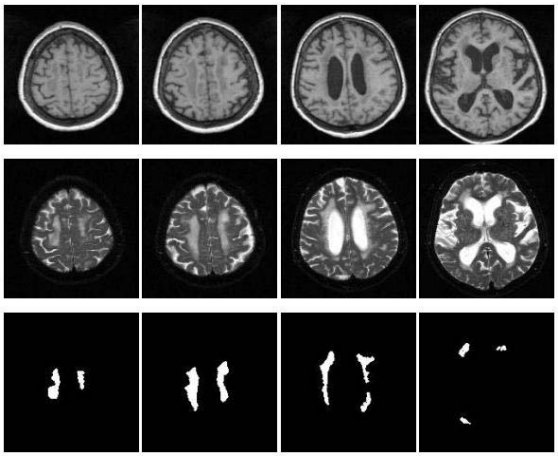

Fig. 2. Original slices and segmented lesions. The first row is the mapped T1 slices; The second row is original T2 slices; And the last row is the segmented lesions.

3.1 Representation of the Discrete Contour Model

In this section, we give a brief description of the original model (refer to [10] for details). The model is made up of a group of vertices connected by edges (see Fig. 3). The position of vertex V_i is represented by vector p_i. The unit vector of the edge between vertex V_i and V_{i+1} is denoted by d_i. The unit tangential vector at vertex i is defined as

$$t_i = \frac{d_{i-1} + d_i}{||d_{i-1} + d_i||} \tag{2}$$

The radial vector r_i is obtained by rotating the tangential vector $\pi/2$ clockwise. Each vertex moves along its radial vector during the deformation. The movement of each vertex is based on the sum of the internal, external, and a damping force. The internal force, which is based on the curvature $c_i = d_i - d_{i-1}$, makes the dynamic contour smooth. The damping force $f_{damp,i}$ is proportional to the

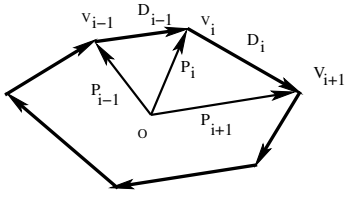

Fig. 3. The model consists of a set of vertices V_i, which are connected by edges D_i.

velocity of the vertex. The contour deformation is computed in discrete positions in time

$$p_i(t + \Delta t) = p_i(t) + v_i(t)\Delta t \tag{3}$$

$$v_i(t + \Delta t) = v_i(t) + a_i(t)\Delta t \tag{4}$$

$$a_i(t + \Delta t) = f_i(t + \Delta t)/m_i \tag{5}$$

$$f_i = w_{ex} f_{ex,i} + w_{in} f_{in,i} + w_{damp} f_{damp,i} \tag{6}$$

where a_i, v_i and m_i are vertex acceleration, velocity and mass, respectively; w_{ex}, w_{in}, and w_{damp} are weights for the external, internal, and damping forces, respectively. For a special application, it is important to define the external force.

3.2 External Forces

For an application of the discrete contour model, it is of great importance to define a proper external force. Our external force includes an edge based component, a balloon component and a shrinking component. Often there are multiple boundaries near the lesions. We assume that the initial contour is placed near the real edge of the lesions. The assumption is true, when the T1 image volume has high resolution along the slice direction and the lesion is not too small. And we also define the balloon and shrinking force to cope with the cases that the assumption is not true. The total external force is:

$$f_{ex,i} = f_{ex,i,ege} + f_{ex,i,bal} + f_{ex,i,shr} \tag{7}$$

- Edge based component: we search the nearest edge in the direction of r_i. The point on this direction can be represented by $p_i + xr_i$. The intensities of the points $p_i + xr_i$ form an function $g(p_i + xr_i)$ with $-L < x < L$, where L is a constant. The nearest edge point is

$$p^\star = p_i + x^\star r_i \tag{8}$$

  where $x^\star$ is the minimum of x, which satisfies $g^{(2)}(p_i + xr_i) = 0$. The edge based component is then calculated by

$$f_{ex,i,ege} = ((p^\star - p_i)\cdot r_i)r_i = x^\star r_i \tag{9}$$

- Balloon component: In some cases, the initial vertex is inside the lesions, so a balloon force is required to let the vertex move outside. We use Γ_i to denote the set made up of vertex i and its four nearest neighbors. if $|I_j - \mu_{les}| < \sigma_{les}$, $j \in \Gamma_i$, then $f_{ex,i,bal} = -\gamma$. Here I_j is the intensity of pixel j; μ_{les} and σ_{les} are the mean value and standard deviation of the lesions, respectively, which are obtained during the lesion segmentation based on both weightings.
- Shrinking component: The initial vertex sometimes locates outside the lesions, therefore we add a shrinking component to let the vertex move inside. if $|I_j - \mu_{les}| > 2\sigma_{les}$, $j \in \Gamma_i$, then $f_{ex,i,shr} = \gamma$.

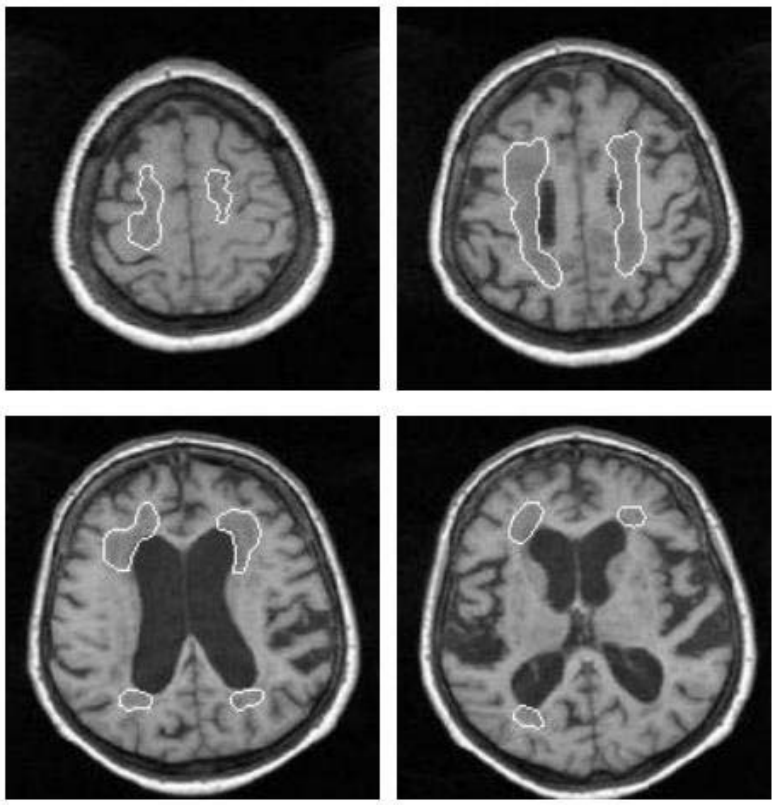

Fig. 4. Some slices of segmented lesions of one patient.

4 Experimental Results

Our experimental image volumes were obtained by a 1.5 Tesla clinical MR scanner. The voxel size of the T1 volume is $0.977 \times 0.977 \times 1$ mm; The T2 volume is $0.498 \times 0.498 \times (5.0 - 7.0)$ mm.

In our experiment, some important parameters are as follows: $\beta = 0.2$, $\Delta = 0.5$, $m_i = 1$, $w_{ex} = 2.5$, $w_{in} = 2$, $w_{damp} = 1$, $L = 5$, $\gamma = 1$. In Fig. 4 and Fig. 5, some slices of the segment results of different patients are displayed, in which the boundaries of the lesions are shown. Validating the extent of the white matter lesions is difficult: Lesion borders are faint, and sometimes the distinction between a lesion and grey matter of a fundus region is hard to draw. Thus, we resort to a critical visual inspection of the results by a neuroradiologist. Note that the caudate nucleus that is similar in intensity to grey matter and is often adjacent to a white matter lesion, is correctly excluded from the lesion area here.

The effect of the internal force is to make the curve smooth. The larger the parameter w_{in}, the smoother the curve. The external force try to let the curve approach the image edges. The final obtained curve is a trade-off between the

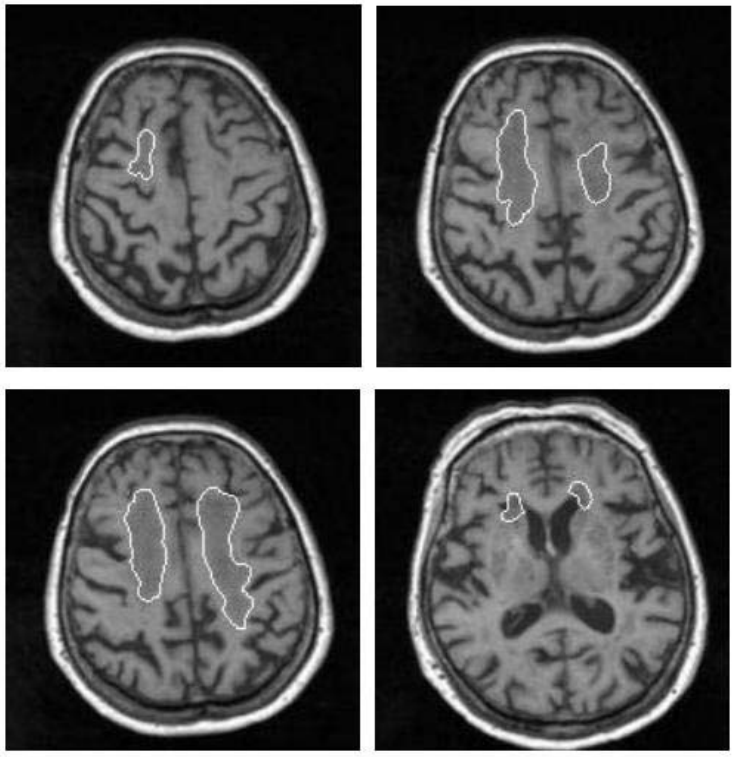

Fig. 5. Some slices of segmented lesions of another patient.

external force and internal force. For our image datasets, the above parameter values are proper. It seems that they are too many parameters. In fact, for a set of image volumes, we can adjust them once and they can be used for all other image volumes. In all of the parameters, the user must adjust β. For our image volumes, $\beta = 0.1 - 0.2$ is proper, which can be seen from Fig. 6. Because the deformable model adapts itself based on the image slices, the result is not sensitive to parameter β.

5 Summary

In this paper, we developed a novel and effective white matter lesion segmentation algorithm. Our method is based on T1 and T2 image volumes. But we do not assume that they have the same resolution. We firstly analyze those T1 slices, which have corresponding T2 slices. The segmented lesions in these slices provide location, shape and intensity statistical information for processing other neighboring T1 slices without corresponding T2 slices. This prior information is used to initialize a discrete contour model in the segmentation of the remaining T1-weighted slices.

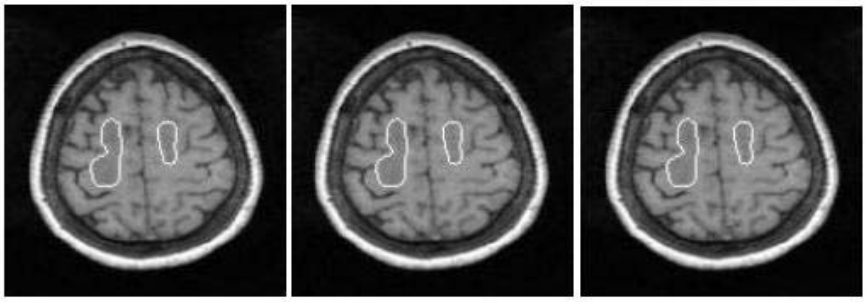

Fig. 6. Effect of parameter β, from left to right $\beta = 0.1$, 0.15, and 0.2, respectively.

References

1. A. P. Zijdenbos, B. M. Dawant, R. A. Margolin, and A. C. Palmer, "Morphometric Analysis of White Matter Lesions in MR Images: Method and Validation", IEEE Trans. Med. Imag., vol. 13, 1994, pp. 716-724.
2. I. Kapouleas, "Automatic Detection of White Matter Lesions in Magnetic Resonance Brain Images", Comput. Methods and programs in Biomed., vol. 32, 1990, pp. 17-35.
3. K. V. Leemput, F. Maes, D. Vandermeulen, A. Colchester, and P. Suetens, "Automated Segmentation of Multiple Sclerosis Lesions by Model Outlier Detection", IEEE Trans. Med. Imag., vol. 20, 2001, pp. 677-688.
4. C. Pachai, Y. M. Zhu, J. Grimaud, M. Hermier, A. Dromigny-Badin, A. Boudraa, G. Gimenez, C. Confavreux, J. C. Froment, "A Pyramidal Approach for Automatic Segmentation of Multiple Sclerosis Lesions in Brain MRI", Computerized Medical Imaging and Graphics, vol. 22, 1998, pp. 399-408.
5. V. A. Kovalev, F. Kruggel, H. J. Gertz, D. Y. V. Cramon, "Three-Dimensional Texture Analysis of MRI Brain Datasets", IEEE Trans. Med. Imag. vol. 20, 2001, pp. 424-433.
6. S. A. Hojjatoleslami, F. Kruggel, and D. Y. von Cramon, "Segmentation of White Matter Lesions from Volumetric MR images", Medical Image Computing and Computer-Assisted Intervention, Lecture Notes in Computer Science, vol. 1679, pp. 52-61, Heidelberg Springer.
7. M. Kamber, R. Shinghal, D. L. Collins, G. S. Francis, and A. C. Evans, "Model-Based 3-D Segmentation of Multiple Sclerosis Lesions in Magnetic Resonance Brain Images", IEEE Trans. Med. Imag., vol. 14, 1995, pp. 442-453.
8. F. Maes, A. Collignon, D. Vandermeulen, G. Marchal, and P. Suetens, "Multimodality Image Registration by Maximization of Mutual Information", IEEE Trans. Med. Imag. vol. 16, 1997, pp. 187-198.
9. M. N. Ahmed, S. M. Yamany, N. Mohamed, A. A. Farag and T. Moriarty, "A Modified Fuzzy C-Means Algorithm for Bias Field Estimation and Segmentation of MRI Data", IEEE Trans. Med. Imag., vol. 21, 2002, pp. 193-199.
10. S. Lobregt, and M. A. Viergever,"A Discrete Dynamic Contour Model", IEEE Trans. Med. Imag., vol. 14, 1995, pp. 12-24.